THE JOURNAL OF PHYSICAL CHEMISTRY C

Article

pubs.acs.org/JPCC

Phenyldithiocarbamate Ligands Decompose During Nanocrystal Ligand Exchange

Andrea M. Munro,*[,‡] Caleb Chandler,[‡] Matthew Garling,[‡] Darick Chai,[‡] Victoria Popovich,[‡] Levi Lystrom,[†] and Svetlana Kilina*[,†]

[‡]Department of Chemistry, Pacific Lutheran University, Tacoma, Washington 98447, United States

[†]Department of Chemistry and Biochemistry, North Dakota State University, Fargo, North Dakota 58108, United States

Supporting Information

ABSTRACT: Exchanging the native surface ligands of CdSe nanocrystals with phenyldithiocarbamate molecules is known to red-shift the absorption spectrum and improve the conductivity of nanocrystal films. However, the mechanism of exchange and the details on the interaction between the nanocrystal surface and phenyldithiocarbamates have not been fully resolved. Using NMR and density functional theory calculations, we show that phenyldithiocarbamates decompose during exchange with native ligands. Phenyldithiocarbamate salts decompose when the cation (triethylammonium in this study) acts as an acid, donating a proton to the 3,5-dimethylphenyldithiocarbamate ligand (DMPTC) producing 3,5-dimethylaniline, carbon disulfide, and other decomposition products. While most decomposition products negligibly interact with the nanocrystal surface, 3,5-dimethylaniline chemically binds to the CdSe nanocrystals. This work demonstrates that the ligand exchange between colloidal nanocrystals and phenyldithiocarbamate ligands occurs in a dynamic system with a variety of molecular species.

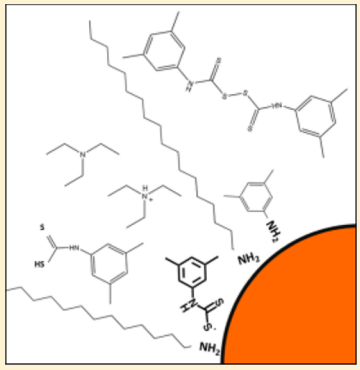

INTRODUCTION

When colloidal semiconductor nanocrystals are incorporated into electronic devices, it is necessary to modify the nanocrystal surface chemistry in order to improve device efficiency.[1−4] The molecules on the surface of a colloidal nanocrystal determine the nanocrystal's solubility, optical properties, and mediate charge transfer to and from the nanocrystal. When nanocrystals are incorporated into photovoltaics, their surface ligands can be substituted either by exchanging the ligands in solution (before processing the nanocrystals into films)[1,2,5] or by treating a nanocrystal film with a solution that contains a new ligand.[6,7] A number of research groups have reported positive changes to the properties of nanocrystal films after the addition of dithiocarbamates.[1,8−11] Weiss et al. reported that the addition of phenyldithiocarbamate (PTC) molecules to CdS, CdSe, and PbS nanocrystals red-shifts the optical band gaps, which they attribute to the delocalization of the photoexcited hole over the nanocrystal and bound PTC ligands.[9,12−14] Zotti et al.[11] found that treating multilayer films of CdSe nanocrystals with bis-dithiocarbamate linkers greatly improved film photoconductivity (by a factor of at least 10−100) compared to films with bis-carboxylate linkers. They found that the photoconductivity of a nanocrystal film treated with a conjugated bis-phenyldithiocarbamate linker was 5× greater than when an unconjugated bis-dithiocarbamate linker was used. When Sargent et al.[1] made photovoltaic devices using films of PbS nanocrystals that had been treated with N-2,4,6-trimethylphenyl-*N*-methyldithiocarbamate ligands, both the device performance and stability in air were improved. Although it has been experimentally confirmed that PTC derivatives improve nanocrystal properties, the details of the ligand exchange process are not fully understood, which poses a challenge to controllable engineering of the nanocrystal surface. In order to fully exploit the beneficial properties of PTC ligands for nanocrystal-based devices, we need a better understanding of the ligand exchange chemistry for this set of ligands.[15,16]

Using NMR and density functional theory (DFT) calculations, we examine the chemistry involved in dithiocarbamate ligand exchange, after the addition of triethylammonium 3,5 dimethyldithiocarbamate (TEA-DMPTC). We performed these experiments using batches of CdSe nanocrystals produced by different methods, in order to ascertain whether the presence of charged X-type ligands or neutral L-type native surface ligands alters the exchange process. TEA-DMPTC is an organic salt, which makes the DMPTC anion an X-type ligand. Negatively charged X-type ligands bind to cadmium atoms on the nanocrystal surface. Conversely, neutral L-type ligands such as primary amines bind to the nanocrystals as Lewis bases by electron pair donation.[15,16] Nanocrystal ligand exchange is usually described by a two-step process in which a native ligand desorbs and the new ligand binds.[15−18] If the new ligand simply replaces the native ligand, it is expected that L-type native ligands can only be replaced by L-type ligands and that X-type native ligands can only be replaced by X-type ligands to maintain charge balance.[15,16]

Received: August 15, 2016
Revised: December 1, 2016
Published: December 2, 2016

DOI: 10.1021/acs.jpcc.6b08247
J. Phys. Chem. C 2016, 120, 29455−29462

EXPERIMENTAL SECTION

Materials. CdO (99%), selenium (100 mesh), tech. grade oleic acid, tech. grade octadecene (ODE), tech. grade (90%) trioctyphosphine oxide (TOPO), 97% octadecylamine (ODA), tributylphosphine (TBP), anhydrous carbon disulfide, ferrocene, and toluene were purchased from Sigma-Aldrich. Acetone, methanol, ethyl acetate, and hexane were purchased from Fischer Scientific. Triethylamine and 3,5-dimethylaniline were purchased from MCB Reagents and Alfa Aesar, respectively. Deuterated solvents d-MeOH, D_2O, and $CDCl_3$, were purchased from Cambridge Isotopes. All chemicals were used as received.

QD Syntheses. *Amine-Capped Nanocrystals.* Nanocrystal spheres were synthesized using the hot-injection method as described by Munro et al.[18] Briefly, CdO (0.077 g, 0.60 mmol) and oleic acid (0.68 g, 2.4 mmol) were added to a 50 mL 3-neck flask, purged with $N_{2(g)}$, and then heated to 180 °C until the solution becomes clear and colorless. The solution is then removed from heat and allowed to cool to room temperature. Next, 0.5 g of 90% TOPO, 1.5 g of ODA, 2.0 g of ODE and a stir bar are added to the flask and it is heated under $N_{2(g)}$. As soon as the solution reaches 270 °C, 1.5 mL of a Se-TBP solution is quickly injected. The Se-TBP stock solution contains selenium shot (0.70 g, 8.9 mmol), TBP (2.3 g, 11 mmol), and ODE (5.8 g). After the Se-TBP solution is injected, the solution is allowed to continue heating at 260 °C for up to 20 min depending on the size of nanocrystal desired.

After the synthesis, all nanocrystal batches were extracted twice with hexanes and methanol in a separatory funnel and then precipitated three times to remove excess ligand from the synthesis. Acetone was used to precipitate the nanocrystals that are resuspended during the washing process with toluene. After removing excess ligands, the nanocrystal spheres were dried and then resuspended in either chloroform or $CDCl_3$.

Oleate-Capped Nanocrystals. Nanocrystal spheres were synthesized using the hot-injection method as described by Fritzinger et al.[19] Briefly, CdO (0.046 g, 0.36 mmol), oleic acid (1.0169 g, 3.6 mmol), and 12 mL of ODE were added to a 50 mL 3-neck flask and then heated to 100 °C under $N_{2(g)}$ and allowed to degas. After being allowed to degas for 1 h, the solution was heated to 250 °C until the solution becomes clear and colorless. Next, the solution is heated while stirring to 265 °C and 3.6 mL of a Se solution is swiftly injected. The Se stock solution is prepared by dissolving selenium shot (0.1263 g, 1.6 mmol) in ODE (16 mL) at 195 °C for 2 h under $N_{2(g)}$. After the Se solution is injected, the solution is allowed to continue heating at 260 °C for up to 20 min depending on the size of nanocrystal desired.

After the synthesis, all nanosphere batches were extracted twice with methanol in a separatory funnel. There was enough excess ODE that no cosolvent needed to be added to the solution. After the extractions, the nanocrystal solution was collected in centrifuge tubes. An excess of methanol was added to each centrifuge tube to continue to remove excess ODE and oleic acid from the nanocrystal solution. This process was repeated until the excess ODE was removed, leaving a nanocrystal pellet behind. After removing excess ligands, the nanocrystal spheres were allowed to dry and then resuspended in either chloroform or $CDCl_3$.

Ligand Synthesis. TEA-DMPTC was synthesized following a procedure described by Nath et al.[20] Briefly, carbon disulfide (1.9 g) and triethylamine (3.03 g) were mixed in an Erlenmeyer flask cooled with an ice-bath. Next, 3,5-dimethylaniline (1.21 g) was added dropwise. The reaction was allowed to stir for 1−2 h during which time salt was observed to precipitate out of solution. The TEA-DMPTC was purified by vacuum filtration using a 95:5 ethyl acetate:hexane solution, then crushed with a mortar and pestle and filtered again, yielding a fine yellow powder. Purifying the TEA-DMPTC prevents decomposition of the salt.

Ligand Exchange Procedure. Ligand exchange was performed by adding 0.10 g of TEA-DMPTC to 2 mL solutions of amine-capped CdSe nanocrystals and 0.20 g of TEA DMPTC with oleate-capped CdSe nanocrystals. The solutions have an absorbance of 2.0−2.8 at the nanocrystal first absorbance peak when measured in a cuvette with a 1 cm path length. After adding TEA-DMPTC, the solutions were mixed well and allowed to react for 10 min in the dark before adding an excess of methanol to precipitate the nanocrystals and remove excess ligand. The mixture was centrifuged at 5000 rpm for 5 min, then the yellow supernate was poured off and the nanocrystals were allowed to dry overnight in a fume hood in the dark. We observe that when ligand exchange is performed with more dilute solutions, that it is difficult to precipitate the nanocrystals from solution. It is also more difficult to resuspend the nanocrystals after exchange. Absorbance measurements were performed using a cuvette with a 1 cm path length in an Agilent 8453 UV−vis spectrometer.

NMR Measurements. H NMR measurements were performed using a 600 MHz Avance Bruker NMR operated with TopSpin 3.2. All 1D H NMR experiments were conducted with 16 scans, TD = 65536, 2 dummy scans, and D1 = 1 s for ligand only samples and D1 = 15 s for samples with nanocrystals. All deuterated solvents were purchased from Cambridge Isotope Laboratories.

Computational Methods. DFT calculations were performed using Gaussian-09 quantum chemistry software.[21] Initial geometries of nanocrystals were constructed from wurtzite crystal structure[22] with an approximately spherical shape of about 1.5 nm diameter resulting in a $Cd_{33}Se_{33}$ nanosystem and then subsequently optimized with DMPTC ligands and their decomposition products at different attachment modes and different concentrations to the lowest energy configuration. Magic-sized $Cd_{33}Se_{33}$ is often taken as a common model of the CdSe nanocrystals in quantum chemistry simulations,[23] because they are the smallest stable nanocrystal experimentally realized,[24,25] while their small size allows for first-principle calculations of their ground and excited state properties.[26−29] The nonstoichiometric $Cd_{34}Se_{33}$ and $Cd_{39}Se_{33}$ structures were created from $Cd_{33}Se_{33}$ by enriching the surface with Cd^{2+} ions. Here we consider the stoichiometric $Cd_{33}Se_{33}$ structures as analogous to the amine-capped nanocrystals and the Cd-enriched structures mimic the oleate-capped nanocrystals, because it has been shown experimentally[15,19] and computationally[8,30,31] that oleate capping results in Cd-enriched nanocrystals, while neutral ligands like primary amines are typically passivating the stoichiometric CdSe nanocrystals.

All geometry optimizations were performed using the hybrid PBE1PBE functional and the mixed LANL2DZ/6-31G* basis set, where 6-31G* is used for ligand atoms and LANL2DZ for Cd and Se atoms. This combination of functional and mixed basis set has previously successfully benchmarked on similar systems[23,26] of CdSe nanocrystals functionalized by primary amines, phosphine oxides, and carboxylate ligands.[30,31] All considered structures were optimized in chloroform and

DOI: 10.1021/acs.jpcc.6b08247
J. Phys. Chem. C 2016, 120, 29455−29462

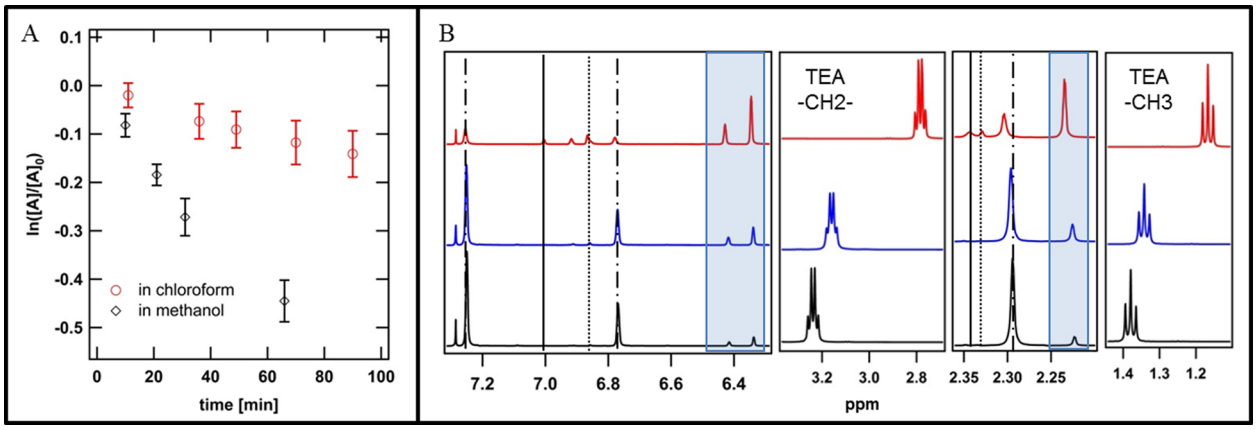

Figure 1. (A) First-order plot of TEA-DMPTC decomposition in $CDCl_3$ (red) and in d-MeOH (black). (B) Kinetics were monitored by H NMR, sample spectra in chloroform are shown at 10 min (black), 70 min (blue), and after 2 days (red). The H NMR peaks associated with TEA shift upfield over time, while the DMPTC signal (dash-dot line) decreases, and the DMA (blue bars) increases. Disulfide (solid line) and protonated DMPTC (dotted line) are observed after long times.

methanol solvents implementing the Conductor Polarized Continuum Model for implicitly included solvent effects. After optimization, the average binding energy (BE) was calculated according to eq 1:

$$B_E = \frac{\text{System}_{\text{Total}} - (QD + n(\text{Ligand}))}{n} \quad (1)$$

where the first term in the numerator is the total energy of the ligated nanocrystal, the second term is the energy of the optimized bare nanocrystal, and the last term is the energy of the optimized pristine ligand. The value n stays for the number of ligands attached to the surface of the nanocrystal. Natural bond orbitals (NBO) calculations were performed within Gaussian-09 to obtain electron density distribution.[32]

RESULTS AND DISCUSSION

Before looking at the ligand exchange process, we examined the stability of the TEA-DMPTC in chloroform (Figure 1) and in methanol. Spectra for the kinetic studies in methanol can be found in the Supporting Information. Although the ligand is stable for multiple months when stored dry on a shelf, TEA-DMPTC decomposes in solution. Dithiocarbamate decomposition is known to occur through complex multistep reactions that involve the protonation of a sulfur atom.[33−35] The triethylammonium deprotonates in solution, causing the H NMR peaks associated with TEA to shift upfield over time[36] (see Figure 1B). At the same time, the 3,5-dithiocarbamate anion breaks into carbon disulfide and 3,5-dimethylaniline (DMA). The TEA-DMPTC and the primary decomposition products are shown in Figure 2. The decomposition occurs 3 times faster in methanol than in chloroform (Figure 1A). Data shown in Figure 1A were fit with a pseudo-first-order integrated rate law to reveal half-lives of 6 h in chloroform and 2 h in methanol. The fast decomposition in methanol is significant, since methanol is often the solvent for dithiocarbamates when ligand exchange in performed on nanocrystals films[11,12] and because we used methanol to precipitate the nanocrystals from solution postexchange in this study. The use of methanol in the ligand exchange process likely reduces experimental reproducibility. Additionally, most studies involving PTCs and nanocrystals[1,9,12,37] have utilized an ammonium cation, which is more acidic than the triethylammonium used in this study.

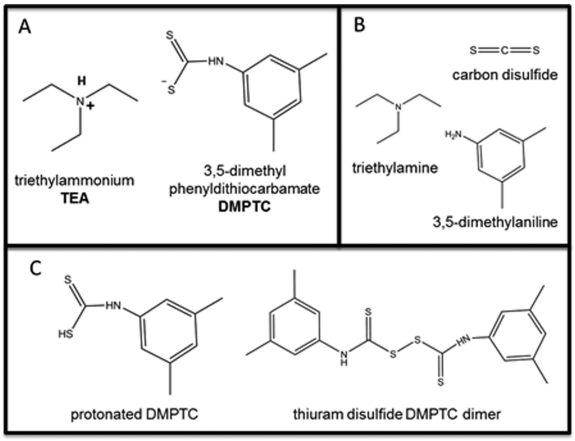

Figure 2. Molecular structure of (A) the cation and anion of triethylammonium 3,5-dimethyldithiocarbamate, (B) decomposition products of both the cation and anion, and (C) additional decomposition products observed by NMR after ligand exchange. The set in panel C is strongly observed in acid-catalyzed decomposition and in the presence of nanocrystals.

The increased acidity of the ammonium cation should increase the rate of ligand decomposition.

Adding TEA-DMPTC to a solution of CdSe nanocrystals causes an immediate red-shift in the nanocrystal absorbance (Supporting Information) and quenches nanocrystal photoluminescence consistent with literature reports.[9,12,37] The H NMR spectra for nanocrystals after exchange with TEA-DMPTC are shown in Figure 3. After the exchange procedure, no TEA is observed in solution. During the exchange procedure, TEA-DMPTC and nanocrystals are allowed to react for 10 min in chloroform and then methanol is added to precipitate the nanocrystals from solution. This precipitation procedure removes the TEA cation as well as excess unbound ligand. Although a number of decomposed species can be seen in Figure 3; we do not observe signal from DMPTC anions. This indicates that the DMPTC anion was either washed away, has completely decomposed, or some fraction is bound to the nanocrystals.[38,39,41−43] We suspect that a fraction of the DMPTC anions bind strongly to the nanocrystals, making their signal unresolvable; a phenomenon that has previously been reported for rigid, strongly bound molecules.[38,39] We note

DOI: 10.1021/acs.jpcc.6b08247
J. Phys. Chem. C 2016, 120, 29455−29462

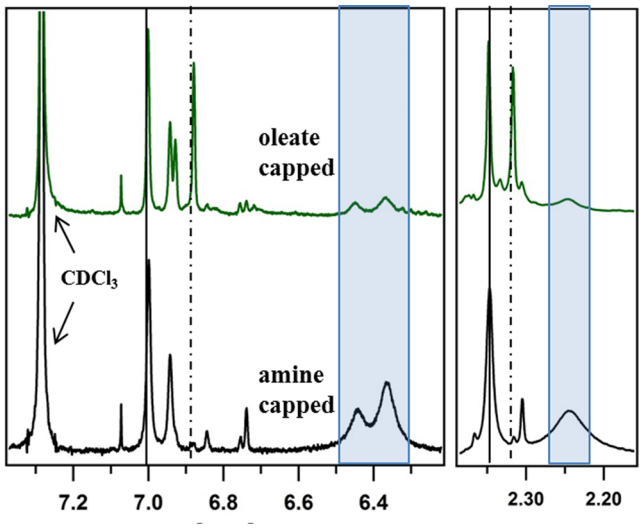

Figure 3. H NMR spectra of nanocrystals after exchange with TEA-DMPTC. We tested batches of nanocrystals that were originally oleate-capped (green) or amine-capped (black). Blue blocks indicate peaks from 3,5-dimethylaniline (DMA). The thiuram disulfide (solid lines) is observed in both samples, while protonated DMPTC (dash-dot line) is a major side product for NCs originally capped with oleate ligands. Signal from the DMPTC anions is not observed.

that there is a small signal near ~6.7 ppm in the spectrum of the amine-capped sample in Figure 3, but this should not be attributed to the presence of the DMPTC anion. The two hydrogens at in the orthoposition of the benzene ring of the DMPTC anion should appear at 7.25 ppm (near $CDCl_3$), while the hydrogen at the paraposition should appear at 6.75 ppm. The absence of signal from the hydrogens at the ortho-position leads us to conclude that the signal near 6.7 ppm for the amine-capped nanocrystal sample does not arise from the DMPTC anion.

In order to examine whether it is reasonable to conclude that some DMPTC anions bind to the nanocrystal becoming unresolvable by H NMR, we performed a titration experiment with three sets of solutions characterized by H NMR (Supporting Information Figure S5). For all samples, the nanocrystal concentration was held constant, while the TEA-DMPTC concentration was varied. For each set, we made a single stock solution with TEA-DMPTC that was spiked with ferrocene. The stock solution was used to make a pristine TEA-DMPTC solution and a solution with TEA-DMPTC and a high concentration of nanocrystals. The two final solutions had the same concentration of TEA-DMTPC and ferrocene. The DMPTC anion signal decreased by 35−75% in the presence of the nanocrystals. This decrease does not correlate with an increase in signal from the decomposition products, but is consistent with the DMPTC anions disappearing upon binding to CdSe nanocrystals. Additional details and the spectra can be found in the Supporting Information. Thus, we conclude that some of the DMPTC that was added to solution is strongly bound to the nanocrystals and is not resolvable because the relaxation time for a bound, rigid small molecule is longer than the time frame for the H NMR experiment. This is consistent with what is observed for longer, floppy ligands that are bound to nanocrystals.[15,19,41−43] For example, the vinyl protons of oleic acid (or oleate) broaden when the ligand is bound to a nanocrystal,[15,19,41] while the first three resonances for alkanethiols bound to metal nanoparticles cannot be resolved by NMR.[42,43]

The broad peaks in Figure 3 at 6.44, 6.37, and 2.24 ppm (shadowed in blue) indicate that DMA binds to the nanocrystal surface after ligand exchange. When nanocrystals are present, the DMA peaks are 5−10 times broader. Notably, DMA (an L-type ligand) appears to bind to the nanocrystals regardless of whether the native surface ligands were neutral L-type amine ligands or charged X-type oleate ligands. Our results are consistent with the report that amines can bind to oleate-capped nanocrystals after displacement of the Z-type Cd-$(oleate)_2$ ligand from Owen et al.[15] The peak broadening decreases in samples with high ligand to nanocrystal ratios, where a larger fraction of the DMA should be unbound. Other species present in the solution are protonated DMPTC and a thiuram disulfide DMPTC dimer (their chemical structures are illustrated in Figure 2C). Both of these molecules are present after a 10 min ligand exchange with nanocrystals, but neither appear to bind. Diffusion-ordered NMR (DOSY) was used to further characterize these samples (see Supporting Information). The DOSY results indicate that the DMA in our samples is weakly bound to the nanocrystal surface, meaning that the DMA is quickly adsorbing and desorbing from the surface. Weak binding of primary amines to CdSe nanocrystals has previously been reported by Hens et al.[40] They observed broadened H NMR peaks for octylamine with a minimal change in the diffusion constant of the bound amine, similar to what we observe in this study.

Interestingly, protonated DMPTC and the dimer are produced quickly when TEA-DMPTC is mixed with the nanocrystals, while neither appear in pristine TEA-DMPTC solution unless the ligand is allowed to decompose for at least 8 h (Figure 1). We note that more protonated DMPTC is produced during ligand exchange with oleate-capped nanocrystals, than for amine-capped nanocrystals. This difference can be explained by a higher concentration of oleic acid in solutions of the oleate-capped nanocrystals. It can be difficult to remove excess oleic acid from solutions of oleate-capped nanocrystals even after repeated washings with methanol. We examined the chemistry between oleic acid and TEA-DMPTC by titrating TEA-DMTPC with the weak acid in the absence of nanocrystals (complete details in the Supporting Information). DMPTC reacts with oleic acid, producing DMA, protonated DMPTC, and the thiuram dimer. It is also possible that DMPTC anion decomposition is catalyzed by the nanocrystals themselves. Dithiocarbamates and thiols can be photo-electrochemically oxidized using CdSe electrodes,[44,45] and recently CdSe nanocrystals were shown to photocatalyze the production of hydrogen and disulfides from thiols bound to the nanocrystal surface.[46] These interesting results indicate that the ligand exchange chemistry of this system is complicated not only by reactions between the TEA-DMPTC cation and anion, but by reactions of the DMPTC anion with weak acids (like oleic acid) in solution and possibly with the nanocrystals themselves.

To gain atomistic insights into the ligand exchange process, DFT calculations were carried out on smaller size models of $Cd_{33}Se_{33}$ of ~1.5 nm in diameter applying the similar approach as has been reported in literature on computational simulations of ligand-nanocrystal interactions and their effects on optoelectronic properties.[27,28,30,47] First, we model the interaction between the $Cd_{33}Se_{33}$ and the protonated and deprotonated DMPTC, its decomposition products, and

DOI: 10.1021/acs.jpcc.6b08247
J. Phys. Chem. C 2016, 120, 29455−29462

acetates (representing the native oleate ligands) by attaching a single molecule of each type at different positions with respect to the nanocrystal surface, as illustrated in Supporting Information Figure S10. For DMPTC, the difference between the nanocrystal-ligand binding energy for the various attachment modes is on the order of thermal fluctuations (Figure S11 in the Supporting Information). This means that there is not a distinct preferential attachment mode for DMPTC to the nanocrystal; the various binding configurations, including monodentate, chelating, and bridging attachments are equally probable under normal conditions (see Supporting Information, Figure S11 and Tables S2−S4). This conclusion is consistent with the results of Car−Parrinello molecular dynamics (CPMD) reported by Azpiroz et al.,[8] where ligands similar to DMPTC have demonstrated their dynamical interaction with the surface of Cd-enriched $Cd_{40}Se_{31}$ nanocrystal, switching between different binding modes along the 5 ps CPMD trajectory. Such a mobile behavior of DMPTC is drastically different from more rigid interactions between the nanocrystal and carboxylate groups, which distinguishably favor the bridging attachment to the CdSe surface.[8,30,48,49]

Figure 4 presents the nanocrystal-ligand binding energies for each molecule calculated as a difference between the total

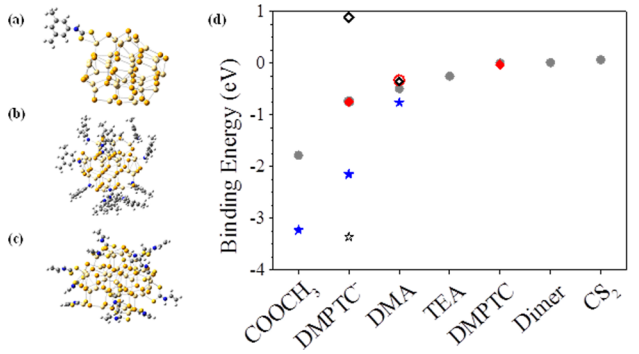

Figure 4. Models of ligated nanocrystal structures and the nanocrystal-ligand binding energies calculated in chloroform: (a) Single 3,5-dimethylaniline (DMA) ligand bound to $Cd_{33}Se_{33}$; (b) fully passivated $Cd_{33}Se_{33}$ by DMA; (c) Cd-enriched $Cd_{39}Se_{33}$ fully passivated with vinyl substituents that are the reduced models of DMA. (d) Average binding energies between the nanocrystal and each ligand. Filled symbols correspond to structures with a single attached ligand, empty symbols are for fully passivated structures. Circles denote $Cd_{33}Se_{33}$ with adsorbed acetate (reduced oleate models), DMPTC, and its decomposition products; diamonds indicate $Cd_{33}Se_{33}$ covered by reduced models of ligands such as vinyl (reduced model for DMA) and vinylthiocarbamate (reduced model for DMPTC); the star corresponds to ligands bound to Cd-enriched nanocrystals (either $Cd_{34}Se_{33}$ when a single molecule is attached or $Cd_{39}Se_{33}$ at full passivation).

energy of the nanocrystal with one adsorbed molecule and the total energy of the optimized isolated ligand and bare nanocrystal (see eq S1 in the Supporting Information) and then averaged over different binding conformations. In the case of multiple ligands at the QD surface, the binding energy is calculated for an individual molecule at its specific site at the nanocrystal facet by taking a difference between the total energy of fully passivated nanocrystal and the same structure with one cut ligand and the isolated ligand (see eq S2 in the Supporting Information). For a single ligand attachment in chloroform (filled symbols in Figure 4), the acetate—a reduced model of the oleate ligand—has the strongest interactions with the stoichiometric $Cd_{33}Se_{33}$, as evidenced by the most negative value of the ligand-nanocrystal binding energy. However, the QD-acetate interaction rapidly diminishes as the number of acetate ligands at the surface increases due to a strong electrostatic repulsion between acetate anions, as has been demonstrated in our previous studies.[30]

Experimental studies conclude that anionic X-type ligands (one-electron donors), such as oleates, typically result in nanocrystals rich in metal cations to balance the charge on the ligands and ensure overall charge neutrality of the nanocrystal.[19,49] Alternatively, recent experiments[15] have demonstrated that the surface layer of excess metal ions can bind to and dissociate from nanocrystal surfaces as carboxylate complexes ($M^{2+}(RCOO^-)_2$), these complexes are known as Z-type ligands (two-electron acceptors). As such, the oleate-ligated CdSe nanocrystals are thought to be a stoichiometric core with a layer of neutral cadmium(II) carboxylate complexes adsorbed to their surfaces.[15,39] However, our recent computational results call into question the correctness of this assumption.[30] As reported in ref 30., the most stable ligated conformations are those where a single acetate is attached to extra Cd^{2+} forming a $[Cd^{2+}(CH_3COO^-)]$ cation at the nanocrystal's surface (the binding geometry is illustrated in Supporting Information, Figure S12). Further stabilization is achieved when the cation complex is accompanied by an acetate anion attachment at the surface, balancing the overall neutral charge of the system and resulting in a 2:1 ratio between acetates and extra Cd ions (Figure S12B). By contrast, attachment of a neutral metal−acetate complex $[Cd^{2+}(CH_3COO^-)_2]$ to the stoichiometric nanocrystal surface is reported to be the least energetically preferable, independent of the degree of ligand passivation and the type of nanocrystal facet.[30] On the other hand, a weak interaction of the $[Cd^{2+}(CH_3COO^-)_2]$ with the nanocrystal leads to its easy detachment from the stoichiometric surface, allowing for neutral L-type ligands (two electron donors) such as primary amines to bind to cadmium sites that have been partially coordinated by carboxylate groups from the Cd(II) complex. Such an indirect substitution between Z- and L-type ligands is in good agreement with the experimental findings of Owen et al.[15]

We have compared the QD−ligand interaction of the cadmium(II) acetate cation and a neutral complex $[Cd^{2+}(CH_3COO^-)_2]$ with the $DMPTC^-$ anion at the $Cd_{33}Se_{33}$. The obtained binding energies are comparable in the case of the $[Cd^{2+}(CH_3COO^-)]$ cation and the $DMPTC^-$ anion. This trend is the most pronounced at the most reactive surfaces having only 2-coordinated Cd ions (Supporting Information, Figure S11B). Based on these calculations, we conclude that there is a small probability of having neutral cadmium-oleate complexes at the nanocrystal surface before the exchange. Instead, a balanced mixture of oleate anions and cadmium(II) oleate cations passivate the nanocrystal surface resulting in overall Cd-enriched nanocrystals. During exchange, some portion of cadmium(II) oleate cations and oleate anions could be substituted by deprotonated DMPTC followed by formation of the neutral cadmium oleate complexes in the solution, which agrees with experimental observations reported in the literature.[39] Because the Z-type $[Cd^{2+}(oleate)_2]$ ligand has a lower binding energy than a $[Cd^{2+}(CH_3COO^-)]$ cation with an oleate anion, we expect that it is energetically favorable for a Cd-enriched nanocrystal to lose a Z-type $[Cd^{2+}(oleate)_2]$

DOI: 10.1021/acs.jpcc.6b08247
J. Phys. Chem. C 2016, 120, 29455−29462

ligand and adsorb an X-type DMPTC anion. It should be noted, however, that an X-type DMPTC anion cannot directly replace a $[Cd^{2+}(oleate)_2]$ ligand on the nanocrystal surface, because $[Cd^{2+}(oleate)_2]$ is displaced from Se^{2-} binding sites, while a DMPTC anion binds to Cd^{2+} surface atoms.

Among the ligands that can be exchanged, the deprotonated DMPTC anion has the most favorable binding to either stoichiometric ($Cd_{33}Se_{33}$) or nonstoichiometric ($Cd_{39}Se_{33}$) nanocrystals. By contrast, protonated DMPTC, the thiuram dimer, and carbon disulfide negligibly interact with the nanocrystal surface via physisorption, having nearly zero binding energy. These findings agree with our NMR results that the DMPTC anions and DMA bind to the CdSe nanocrystals and that the DMPTC anion should form a stronger bond than DMA to the nanocrystal surface. Interestingly, changing the solvent from chloroform to methanol significantly weakens the interaction between the nanocrystal and the DMPTC- anion (see Supporting Information, Figure S13). This is a common trend[26,27] since the considered systems have a strong electrostatic dipole moment that is screened out by a polar solvent. Nonetheless, the ligand-nanocrystal binding energy is still negative and about 3 times larger than the thermal energy (Table S3, Supporting Information), pointing to DMPTC anions staying bound to the nanocrystal surface when precipitated in methanol.

Although useful, structures with a single molecule adsorbed at the nanocrystal do not present a complete picture of surface passivation, where steric and electrostatic interactions between neighboring ligands can significantly affect nanocrystal-ligand interactions. As such, we consider structures where 12 molecules of deprotonated DMPTC and DMA are attached to available surface cadmiums at the $Cd_{33}Se_{33}$ model. To reduce computational cost, we substitute the phenyl ring in DMPTC and DMA with the vinyl group. Analysis of NBOs indicates that the reduced models have a negligible impact on the electron density distribution, the geometry of the ligated nanocrystal, and the nanocrystal-ligand binding energy (Supporting Information, Figure S14). In fact, the binding energy between the $Cd_{33}Se_{33}$ and a single DMPTC in its protonated and deprotonated forms is identical to those of the reduced ligand (filled red diamonds in Figure 4).

For neutral DMA ligands, the strength of the ligand-nanocrystal interaction is only slightly decreased for the full surface passivation (empty black diamonds in Figure 4) compared to the single DMA molecule adsorbed at the $Cd_{33}Se_{33}$ both for the realistic (empty black diamonds in Figure 4) and reduced ligand models (empty red circles for vinyl in Figure 4). By contrast, strong electrostatic and steric repulsion between deprotonated DMPTC ligands drastically reduces the nanocrystal-ligand interaction, resulting in positive binding energies and, consequently, unbound DMPTC anions from the stoichiometric $Cd_{33}Se_{33}$. This effect is expected to be less pronounced in larger nanocrystals with a smaller surface to volume ratio, where anionic ligands can be located further from each other. Overall, significant weakening of their binding to the nanocrystal with increasing DMPTC concentration brings us to the conclusions that DMPTC anions can passivate the stoichiometric nanocrystals only at some limited amount. However, the interaction between the nanocrystal and the DMPTC ion remains strong in the presence of small ligands, such as primary amine or carboxylates (Table S5, Supporting Information). As such, we can conclude that DMPTC anions likely do not cover all reactive surface sites of the nanocrystals, most of these sites still have native ligands bound, such as primary amines (for stoichiometric nanostructures) or carboxylate derivatives (for Cd-enriched nanocrystals) with some contribution from the dissociated product DMA. This is consistent with our NMR observations that native ligands remain bound even after ligand exchange.

We further examine the difference in binding energies for the DMPTC anions when bound to $Cd_{33}Se_{33}$ (stoichiometric) and $Cd_{39}Se_{33}$ (Cd-enriched) nanocrystals. We consider the $Cd_{33}Se_{33}$ structure to be analogous to the amine-capped nanocrystals, and the $Cd_{39}Se_{33}$ structure is analogous to the oleate-capped structure, because it was shown both experimentally[50] and computationally[30] that oleate capping results in Cd-enriched nanocrystals, while neutral ligands like primary amines are typically passivating the stoichiometric surfaces of CdSe nanocrystals. Calculations of Cd^{2+}-enriched $Cd_{39}Se_{33}$ nanostructures covered by 12 vinylthiocarbamate anions (the reduced models of DMPTC anions) show a dramatic increase in the ligand-nanocrystal interactions in the chloroform (star symbols in Figure 4), as compared to those of the stoichiometric ($Cd_{33}Se_{33}$) nanocrystals. This can be rationalized by considering the overall neutrality of the system, where positively charged cadmium cations and anionic ligands compensate each other and stabilize the energy of the ligated Cd-rich nanocrystal. As such, one might expect that DMPTC anion binding should be more efficient for oleate-passivated nanocrystals, compared to amine-ligated structures. Experimentally, however, we do not observe much difference between the two types of nanocrystals. This is because the DMPTC anions bind to the nanocrystal surface only in small amounts, since the strong electrostatic and steric repulsions between bulky DMPTC ions hinder their interactions with the nanocrystal surface. Additionally, the interaction of the nanocrystal with carboxylate groups is much stronger than with amine ligands (Figure 4), implying that exchange of the oleate ligands with DMTPC anions is less favorable thermodynamically than with amine ligands. Overall, the interplay of both factors causes the final nanocrystal structures to have a small amount of DMPTC anions and their dissociation products (mostly DMA) and some amount of native ligands bound after the exchange. Because of these mixtures, nanocrystals that were initially amine-capped or oleate-capped demonstrate no significant differences in their NMR spectra, as observed.

CONCLUSIONS

We found that after ligand exchange with TEA-DMTPC, there are a variety of ligands bound to the nanocrystal surface. Our experimental and computational results provide evidence that ligand exchange is much more complicated than the traditional mass action ligand exchange picture.[6,15,16] Our study indicates that when an X-type ligand has an acidic cation, that side reactions can compete with the ligand exchange process. The presence of multiple ligand species in solution that can react creates a more dynamic picture[16] than the traditional view of a native ligand simply desorbing and being replaced by a new ligand that is present in large excess. We have found evidence for two phenomena: (1) acid−base chemistry between the anion and cation of X-type ligands and (2) the conversion of dithiocarbamate ligands to thiurum disulfides in solution. Our results are consistent with observations by Balazs et al.[6] that cation acidity can influence the degree of ligand exchange in nanocrystal films. Additionally, we have examined which

DOI: 10.1021/acs.jpcc.6b08247
J. Phys. Chem. C 2016, 120, 29455−29462

chemical reactions occur in this system. This work demonstrates the importance of characterizing the extent of ligand exchange when developing an exchange protocol. Researchers should consider whether ligand exchange should be performed on nanocrystal films or in solution, the amount of light exposure, and potential side reactions that may affect the exchange process or have consequences for the long-term stability of nanocrystal-based photovoltaics that incorporate PTCs.

■ ASSOCIATED CONTENT

Supporting Information

The Supporting Information is available free of charge on the ACS Publications website at DOI: 10.1021/acs.jpcc.6b08247.

Additional experimental details, computational results, NMR spectra, DOSY spectra, UV−vis absorbance spectra, and TEM images of nanocrystals (PDF)

■ AUTHOR INFORMATION

Corresponding Authors

*E-mail: munroam@plu.edu. Telephone: +1 (253) 538-6393.
*E-mail: svetlana.kilina@ndsu.edu. Telephone: +1 (701) 231-5622.

ORCID

Andrea M. Munro: 0000-0001-7669-350X

Author Contributions

The manuscript was written through contributions of all authors. All authors have given approval to the final version of the manuscript.

Notes

The authors declare no competing financial interest.

■ ACKNOWLEDGMENTS

A.M.M. gratefully acknowledges financial support from the M. J. Murdock Charitable Trust (2009184:JVA:11/19/2009) as well as funding from Pacific Lutheran University through a Karen Hillle Phillips Regency Advancement Award and the Natural Sciences Summer Undergraduate Research Program. A.M.M. thanks Ellen Lavoie for taking TEM images of nanocrystals before and after ligand exchange. TEM imaging was conducted at the Molecular Analysis Facility, which is supported in part by funds from the University of Washington, the Molecular Engineering & Sciences Institute, the Clean Energy Institute, the National Science Foundation and the National Institutes of Health. S.K. acknowledges financial support of the DOE Early Career Research grant DE-SC008446. For computational resources and administrative support, authors thank the Center for Computationally Assisted Science and Technology (CCAST) at North Dakota State University and the National Energy Research Scientific Computing Center (NERSC) allocation award 86678, supported by the Office of Science of the DOE under Contract No. DE-AC02-05CH11231. For partial financial support of the quantum chemistry software, authors acknowledge Sloan Research Fellowship BR2014-073.

■ ABBREVIATIONS

PTC, phenyldithiocarbamate; DMPTC, 3,5-dimethylphenyldithiocarbamate; TEA, triethylammonium; DFT, density functional theory; NBO, natural bond orbital; DMA, 3,5-dimethylaniline

■ REFERENCES

(1) Debnath, R.; Tang, J.; Barkhouse, D. A.; Wang, X.; Pattantyus-Abraham, A. G.; Brzozowski, L.; Levina, L.; Sargent, E. H. Ambient-Processed Colloidal Quantum Dot Solar Cells via Individual Pre-Encapsulation of Nanoparticles. *J. Am. Chem. Soc.* **2010**, *132*, 5952−5953.

(2) Greenham, N. C.; Peng, X.; Alivisatos, A. P. Charge Separation and Transport in Conjugated-Polymer/Semiconductor-Nanocrystal Composites Studied by Photoluminescence Quenching and Photoconductivity. *Phys. Rev. B: Condens. Matter Mater. Phys.* **1996**, *54*, 17628−17637.

(3) Kovalenko, M. V.; Manna, L.; Cabot, A.; Hens, Z.; Talapin, D. V.; Kagan, C. R.; Klimov, V. I.; Rogach, A. L.; Reiss, P.; Milliron, D. J.; et al. Prospects of Nanoscience with Nanocrystals. *ACS Nano* **2015**, *9*, 1012−1057.

(4) Kramer, I. J.; Sargent, E. H. The Architecture of Colloidal Quantum Dot Solar Cells: Materials and Devices. *Chem. Rev.* **2014**, *114*, 863−881.

(5) Dubois, F.; Mahler, B.; Dubertret, B.; Doris, E.; Mioskowski, C. A Versatile Strategy for Quantum Dot Ligand Exchange. *J. Am. Chem. Soc.* **2007**, *129*, 482−483.

(6) Balazs, D. M.; Dirin, D. N.; Fang, H.-H.; Protesescu, L.; ten Brink, G. H.; Kooi, B. J.; Kovalenko, M. V.; Loi, M. A. Counterion-Mediated Ligand Exchange for PbS Colloidal Quantum Dot Superlattices. *ACS Nano* **2015**, *9*, 11951−11959.

(7) Barkhouse, D. A. R.; Pattantyus-Abraham, A. G.; Levina, L.; Sargent, E. H. Thiols Passivate Recombination Centers in Colloidal Quantum Dots Leading to Enhanced Photovoltaic Device Efficiency. *ACS Nano* **2008**, *2*, 2356−2362.

(8) Azpiroz, J. M.; De Angelis, F. Ligand Induced Spectral Changes in CdSe Quantum Dots. *ACS Appl. Mater. Interfaces* **2015**, *7*, 19736−19745.

(9) Frederick, M. T.; Amin, V. A.; Cass, L. C.; Weiss, E. A. A Molecule to Detect and Perturb the Confinement of Charge Carriers in Quantum Dots. *Nano Lett.* **2011**, *11*, 5455−5460.

(10) Teunis, M. B.; Dolai, S.; Sardar, R. Effects of Surface-Passivating Ligands and Ultrasmall CdSe Nanocrsytal Size on the Delocalization of Exciton Confinement. *Langmuir* **2014**, *30*, 7851−7858.

(11) Zotti, G.; Vercelli, B.; Berlin, A.; Virgili, T. Multilayers of CdSe Nanocrystals and Bis(dithiocarbamate) Linkers Displaying Record Photoconduction. *J. Phys. Chem. C* **2012**, *116*, 25689−25693.

(12) Frederick, M. T.; Amin, V. A.; Swenson, N. K.; Ho, A. Y.; Weiss, E. A. Control of Excitation Confinement in Quantum Dot-Organic Complexes through Energetic Alignment of Interfacial Orbitals. *Nano Lett.* **2013**, *13*, 287−292.

(13) Frederick, M. T.; Amin, V. A.; Weiss, E. A. Optical Properties of Strongly Coupled Quantum Dot-Ligand Systems. *J. Phys. Chem. Lett.* **2013**, *4*, 634−640.

(14) Morris-Cohen, A. J.; Malicki, M.; Peterson, M. D.; Slavin, J. W. J.; Weiss, E. A. Chemical, Structural, and Quantitative Analysis of the Ligand Shells of Colloidal Quantum Dots. *Chem. Mater.* **2013**, *25*, 1155−1165.

(15) Anderson, N. C.; Hendricks, M. P.; Choi, J. J.; Owen, J. S. Ligand Exchange and the Stoichiometry of Metal Chalcogenide Nanocrystals: Spectroscopic Observation of Facile Metal-Carboxylate Displacement and Binding. *J. Am. Chem. Soc.* **2013**, *135*, 18536−18548.

(16) De Roo, J.; Ibanez, M.; Geiregat, P.; Nedelcu, G.; Walravens, W.; Maes, J.; Martins, J. C.; Van Driessche, I.; Kovalenko, M. V.; Hens, Z. Highly Dynamic Ligand Binding and Light Absorption Coefficient of Cesium Lead Bromide Perovskite Nanocrystals. *ACS Nano* **2016**, *10*, 2071−2081.

(17) Donakowski, M. D.; Godbe, J. M.; Sknepnek, R.; Knowles, K. E.; Olvera de la Cruz, M.; Weiss, E. A. A Quantitative Description of the Binding Equilibria of para-Substituted Aniline Ligands and CdSe Quantum Dots. *J. Phys. Chem. C* **2010**, *114*, 22526−22534.

(18) Munro, A. M.; Jen-La Plante, I.; Ng, M. S.; Ginger, D. S. Quantitative Study of the Effects of Surface Ligand Concentration on

DOI: 10.1021/acs.jpcc.6b08247
J. Phys. Chem. C 2016, 120, 29455−29462

CdSe Nanocrystal Photoluminescence. *J. Phys. Chem. C* **2007**, *111*, 6220−6227.
(19) Fritzinger, B.; Capek, R. K.; Lambert, K.; Martins, J. C.; Hens, Z. Utilizing Self-Exchange To Address the Binding of Carboylic Acid Ligands to CdSe Quantum Dots. *J. Am. Chem. Soc.* **2010**, *132*, 10195−10201.
(20) Nath, J.; Patel, B. K.; Jamir, L.; Sinha, U. B.; Satyanarayana, K. V. V. V. A One-Pot Preparation of Cyanamide from Dithiocarbamate Using Molecular Iodine. *Green Chem.* **2009**, *11*, 1503−1506.
(21) Frisch, M. J.; Trucks, G. W.; Schlegel, H. B.; Scuseria, G. E.; Robb, M. A.; Cheeseman, J. R.; Scalmani, G.; Barone, V.; Mennucci, B.; Petersson, G. A.; et al. *Gaussian 09*; Gaussian, Inc.: Wallingford, CT, 2009.
(22) Freeman, D.; Mair, S.; Barnea, Z. The Structure and Bijvoet Ratios of Cadmium Selenide. *Acta Crystallogr., Sect. A: Cryst. Phys., Diffr., Theor. Gen. Crystallogr.* **1977**, *33*, 355−359.
(23) Kilina, S.; Kilin, D.; Tretiak, S. Light-Driven and Phonon-Assisted Dynamics in Organic and Semicondutor Nanostructures. *Chem. Rev.* **2015**, *115*, 5929−5978.
(24) Dolai, S.; Nimmala, P. R.; Mandal, M.; Muhoberac, B. B.; Dria, K.; Dass, A.; Sardar, R. Isolation of Bright Blue Light-Emitting CdSe Nanocrystals with 6.5 kDa Core in Gram Scale: High Photoluminescence Efficieincy Controlled by Surface Ligand Chemistry. *Chem. Mater.* **2014**, *26*, 1278−1285.
(25) Wang, Y.; Zhang, Y.; Wang, F.; Giblin, D. E.; Hoy, J.; Rohrs, H. W.; Loomis, R. A.; Buhro, W. E. The Magic-Size Nanocluster $(CdSe)_{34}$ as a Low-Temperature Nucleant for Cadmium Selenide Nanocrystals: Room-Temperature Growth of Crystalline Quantum Platelets. *Chem. Mater.* **2014**, *26*, 2233−2243.
(26) Albert, V. V.; Ivanov, S. A.; Tretiak, S.; Kilina, S. V. Electronic Structure of Ligated CdSe Clusters: Dependence on DFT Methodology. *J. Phys. Chem. C* **2011**, *115*, 15793−15800.
(27) Fischer, S. A.; Crotty, A. M.; Kilina, S. V.; Ivanov, S. A.; Tretiak, S. Passivating Ligand and Solvent Contributions to the Electronic Properties of Semiconductor Nanocrystals. *Nanoscale* **2012**, *4*, 904−914.
(28) Kilina, S.; Ivanov, S.; Tretiak, S. Effect of Surface Ligands on Optical and Electronic Spectra of Semiconductor Nanoclusters. *J. Am. Chem. Soc.* **2009**, *131*, 7717−7726.
(29) Kuznetsov, A. E.; Beratan, D. N. Structural and Electronic Properties of Bare and Capped Cd33Se33 and Cd33Te33 Quantum Dots. *J. Phys. Chem. C* **2014**, *118*, 7094−7109.
(30) Tamukong, P. K.; Peiris, W. D. N.; Kilina, S. Computational Insights into CdSe Quantum Dots' Interactions with Acetate Ligands. *Phys. Chem. Chem. Phys.* **2016**, *18*, 20499−20510.
(31) Sluydts, M.; De Nolf, K.; Van Speybroeck, V.; Cottenier, S.; Hens, Z. Ligand Addition: Energies and the Stoichiometry of Colloidal Nanocrystals. *ACS Nano* **2016**, *10*, 1462−1474.
(32) Reed, A. E.; Curtiss, L. A.; Weinhold, F. Intermolecular Interactions from a Natural Bond Orbital, Donor-Acceptor Viewpoint. *Chem. Rev.* **1988**, *88*, 899−926.
(33) Humeres, E.; Debacher, N. A.; de S. Sierra, M. M.; Franco, J. D.; Schutz, A. Mechanisms of Acid Decomposition of Dithiocarbamates. 1. Alkyl Dithiocarbamates. *J. Org. Chem.* **1998**, *63*, 1598−1603.
(34) Humeres, E.; Debacher, N. A.; Franco, J. D.; Lee, B. S.; Martendal, A. Mechanisms of Acid Decomposition of Dithiocarbamates. 3. Aryldithiocarbamates and Torsional Effects. *J. Org. Chem.* **2002**, *67*, 3662−3667.
(35) Joris, S. J.; Aspila, K. I.; Chakrabarti, C. L. On the Mechanism of Decomposition of Dithiocarbamates. *J. Phys. Chem.* **1970**, *74*, 860−865.
(36) Gift, A. D.; Stewart, S. M.; Bokashanga, P. K. Experimental Determination of pKa Values by Use of NMR Chemical Shifts, Revisited. *J. Chem. Educ.* **2012**, *89*, 1458−1460.
(37) Jin, S.; Harris, R. D.; Lau, B.; Aruda, K. O.; Amin, V. A.; Weiss, E. A. Enhanced Rate of Radiative Decay in CdSe Quantum Dots upon Adsorption of an Exciton-Delocalizing Ligand. *Nano Lett.* **2014**, *14*, 5323−5328.
(38) Amin, V. A.; Aruda, K. O.; Lau, B.; Rasmussen, A. M.; Edme, K.; Weiss, E. A. Dependence of the Band Gap of CdSe Quantum Dots on the Surface Coverage and Binding Mode of an Exciton-Delocalizing Ligand, Methylthiophenolate. *J. Phys. Chem. C* **2015**, *119*, 19423−19429.
(39) Harris, R. D.; Amin, V. A.; Lau, B.; Weiss, E. A. Role of Interligand Coupling in Determining the Interfacial Electronic Structure of Colloidal CdS Quantum Dots. *ACS Nano* **2016**, *10*, 1395−1403.
(40) Hassinen, A.; Moreels, I.; de Mello Donega, C.; Martins, J. C.; Hens, Z. Nuclear Magnetic Resonance Spectroscopy Demonstrating Dynamic Stabilization of CdSe Quantum Dots by Alkylamines. *J. Phys. Chem. Lett.* **2010**, *1*, 2577−2581.
(41) Hens, Z.; Martins, J. C. A Solution NMR Toolbox for Characterizing the Suface Chemistry of Colloidal Nanocrystals. *Chem. Mater.* **2013**, *25*, 1211−1221.
(42) Badia, A.; Gao, W.; Singh, S.; Demers, L.; Cuccia, L.; Reven, L. Structure and Chain Dynamics of Alkanethiol-Capped Gold Colloids. *Langmuir* **1996**, *12*, 1262−1269.
(43) Marbella, L. E.; Millstone, J. E. NMR Techniques for Noble Metal Nanoparticles. *Chem. Mater.* **2015**, *27*, 2721−2739.
(44) Natan, M. J.; Thackeray, J. W.; Wrighton, M. S. Interaction of Thiols with n-Type Cadmium Sulfide and n-Type Cadmium Selenide in Aqueous Solutions: Adsorption of Thiolate Anion and Efficient Photoelectrochemical Oxidation to Disulfides. *J. Phys. Chem.* **1986**, *90*, 4089−40098.
(45) Thackeray, J. W.; Natan, M. J.; Ng, P.; Wrighton, M. S. Interaction of Diethyldithiocarbamate with n-Type Cadmium Sulfide and Cadmium Selenide: Efficient Photoelectrochemical Oxidation to the Disulfide and Flat-Band Potential of the Semiconductor as a Function of Adsorbate Concentration. *J. Am. Chem. Soc.* **1986**, *108*, 3570−3577.
(46) Li, X.-B.; Li, Z.-J.; Gao, Y.-J.; Meng, Q.-Y.; Yu, S.; Weiss, R. G.; Tung, C.-H.; Wu, L.-Z. Mechanistic Insights into the Interface-Directed Transformation of Thiols into Disulfides and Molecular Hydrogen by Visible-Light Irradiation of Quantum Dots. *Angew. Chem., Int. Ed.* **2014**, *53*, 2085−2089.
(47) Kilina, S.; Cui, P.; Fischer, S. A.; Tretiak, S. Conditions for Directional Charge Transfer in CdSe Quantum Dots Functionalized by Ru(II) Polypyridine Complexes. *J. Phys. Chem. Lett.* **2014**, *5*, 3565−3576.
(48) Koposov, A. Y.; Cardolaccia, T.; Albert, V.; Badaeva, E.; Kilina, S.; Meyer, T. J.; Tretiak, S.; Sykora, M. Formation of Assemblies Comprising Ru-Polypyridine Complexes and CdSe Nanocrystals Studied by ATR-FTIR Spectroscopy and DFT Modeling. *Langmuir* **2011**, *27*, 8377−8383.
(49) Hedrick, M.; Mayo, M. L.; Badaeva, E.; Kilina, S. First Principle Studies of the Ground and Excited State Properties of Quantum Dots Functionalized by Ru(II)-Polybipyridine. *J. Phys. Chem. C* **2013**, *117*, 18216−18224.
(50) Weiss, E. A. Organic Molecules as Tools To Control the Growth, Surface Structure, and Redox Activity of Colloidal Quantum Dots. *Acc. Chem. Res.* **2013**, *46*, 2607−2615.

DOI: 10.1021/acs.jpcc.6b08247
J. Phys. Chem. C 2016, 120, 29455−29462